MICROFLUIDIC DEVICE FOR DETERMINING PREFERENTIAL CELL MIGRATION TOWARD EXTRACELLULAR MATRIX PROTEINS

by

NEIL HALL

Presented to the Faculty of the Graduate School of

The University of Texas at Arlington in Partial Fulfillment

of the Requirements

for the Degree of

MASTER OF SCIENCE IN BIOMEDICAL ENGINEERING

THE UNIVERSITY OF TEXAS AT ARLINGTON

MAY 2013

Acknowledgements

Throughout my time as a research assistant, many people such as my mentors, professors, colleagues, family, and friends have influenced me. I would like to thank my mentor and P.I. Dr. Young-tae Kim for helping and guiding me throughout my undergraduate and graduate experience at UT Arlington. He allowed me to pursue my goals in the field of bioengineering research and always encouraged and helped me in every situation. Since I joined him lab in 2009, we have grown to know each other very well, and I would like to thank him for all his support and for challenging me when I thought I could not accomplish my goals.

I would also like to thank the professors of the bioengineering department for serving as my instructors throughout my education process. I have learned valuable research and life experiences, and would like to take this opportunity to thank them. In particular, I am most grateful to Dr. Kytai Truong Nguyen and Dr. George Alexandrakis for serving on my thesis defense committee.

I would like to thank the other members of my lab, my colleagues throughout the years, who have helped me learn and have supported me with my research. Namely, I would like to thank Srikanth Vasudevan, Kailash Karthikeyan, Shreevidhya Banda, Shruti Kanakia, Chetan Bhuwania, and Deepika Tamuly.

Finally, I would like to thank my mother, Mojgan Hall, and my two brothers, Justin and Joshua Hall, for having faith in me and supporting me through my life. They have helped me pave the way toward my goals and my master's degree.

Funding for this research project was provided by UTA (Nano-bio Cluster Program).

April 16, 2013

Abstract

MICROFLUIDIC DEVICE FOR DETERMINING PREFERENTIAL CELL MIGRATION TOWARD EXTRACELLULAR MATRIX PROTEINS

Neil Hall, M.S.

The University of Texas at Arlington, 2013

Supervising Professor: Young-tae Kim

Extracellular matrix (ECM) proteins interact with cells in bodily microenvironments by influencing their essential cellular processes in growth, survival, migration and repair after injury. In this study, a novel microfluidic device was developed to study preferential interactions of cells with multiple extracellular matrix proteins simultaneously in an unbiased manner. The implementation of PDITC-treated glass and a controlled laminar flow of multiple separated, soluble proteins was used to create an unbiased microenvironment in which ECM proteins are adsorbed on the glass surface in a manner that simultaneously exposes cells to multiple proteins, and allows them to migrate or outgrow toward the most growth-promoting “preference” protein. The technique was proved by exposing cortical neurons to laminin and aggrecan simultaneously. The cortical neurons consistently migrated toward the laminin opposed to the aggrecan, which is expected. At this point, different strains of human-derived primary glioblastoma multiforme (GBM) cells were exposed to different proteins and compared for preferential migration differences. One strain (133P) was exposed to two different growth-promoting proteins, laminin and fibronectin, and was found to not have a significant preference towards either when comparing average number of cells migrated. When the data was normalized by percentage, the 133P cells showed a statistically

significant preference toward laminin. A second strain (C419) was tested with laminin, fibronectin, and vitronectin, showing 100% migration towards Laminin in every trial. These results lead to certain conclusions regarding the migration and infiltration patterns of GBM *in vivo* within the healthy brain tissue of patients. With this test platform presented, any strain of cells can be tested for migration preference and patterns, leading to understanding of their growth patterns *in vivo*.

Table of Contents

List of Illustrations

List of Tables

Chapter 1

Introduction

1.1 Microfluidics

Microfluidics is a term that refers to a technology that has recently developed tremendously to aid in many fields of research. The main idea behind microfluidics is solving problems that would otherwise be difficult with larger assays by miniaturizing the techniques and test platforms [1, 2]. This miniaturization, in micron scale, leads to significant advantages in research, such as a smaller requirement of reagents, mass production in a relatively small amount of time and space, faster reactions, and overall cost reduction [2]. Various applications of microfluidics include creation of arrays to study cell-cell interactions and cell-biomolecule interactions, formation of chemical gradients, studying single cells or small clusters of cells, and fabrication of medical diagnostics and biosensors [1, 3, 4]. Typically microfluidic devices are formed by etching the desired pattern into poly(dimethylsiloxane) (PDMS) by creation of a master mold on a silicone wafer. Once this device has been fabricated, it can be attached to glass and manipulated accordingly for ideal experimentation. PDMS is the most widely used platform for microfluidic devices due to its unique and ideal properties as a polymer, including inert behavior, ideal optical transparency, simple fabrication, and low cost [5, 6]. Due to the Si-(CH_3) groups present on the PDMS surface, it exhibits high hydrophobicity, which makes use in microfluidic devices near impossible without surface modifications [7]. Common surface modification techniques to create hydrophilic PDMS surfaces include oxygen plasma, UV treatment, and corona discharge. Oxygen plasma treatment is generally known to be the most effective of the techniques and is accomplished by releasing a concentrated dose of high-energy particles such as electrons, radicals, and ions that oxidize the surface to contain Si-(OH) groups, known as silanol functional groups [7]. It

has been shown that the hydrophilic surface created by oxygen plasma treatment reverts back to a hydrophobic surface within hours if not exposed to a liquid environment [8]. Due to these characteristics and established applications, PDMS microfluidic devices are ideal for culture and analysis of cells *in vitro*.

1.2 PDITC glass treatment

p-Phenylene diisothiocyanate (PDITC) is a compound that is typically used as a chemical crosslinker [9, 10]. Different variations of the protocol for binding PDITC to glass surfaces have been utilized for immobilization of aptamers and oligonucleotides [9, 10, 11]. Typically, after the glass is activated by oxygen plasma treatment to present silanol groups, it is treated with Aminopropyltrimethoxysilane (APTES) to create amino functional groups. The glass is then treated with PDITC to add phenylisothiocyanate groups to the amino groups, which allows for covalent bonding to amino groups. When trying to bind a protein to a glass surface, due to its amino acid framework, this technique allows for a stronger, more permanent bonding. Previous research has demonstrated the ability to bind proteins to glass in the presence of a flow of proteins via the crosslinking protein PLL, but the PLL had to adsorb overnight and the flow process took at least 6 hours [13]. The process of treating glass with PDITC takes roughly 6 hours and the flow of proteins takes 4 hours. Figure 1.1 gives graphical representation of the chemical structures involved with PDITC treatment.

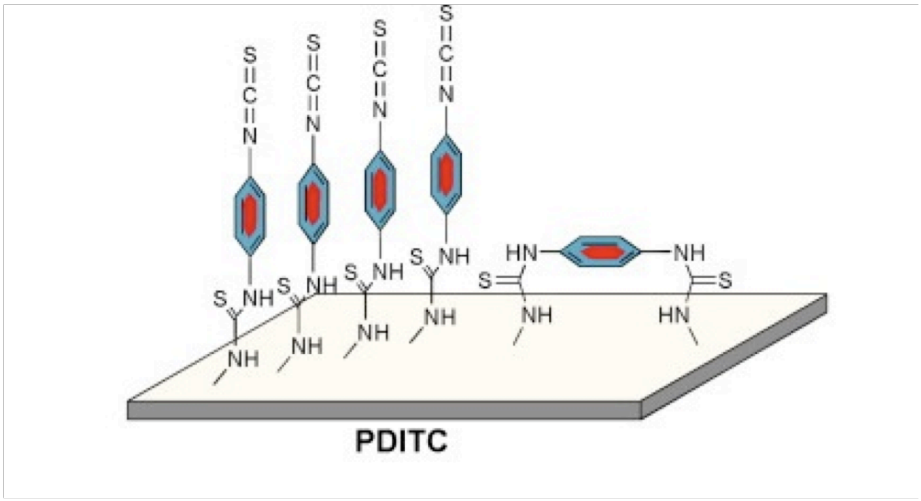

Figure 1.1 Chemical structure of PDITC treated glass [12].

1.3 Extracellular matrix proteins and the brain

The extracellular matrix is a network of molecules that act primarily to support cells and tissue in the body [14]. It is a large component of connective tissue and is divided into the interstitial matrix and basement membrane. The interstitial matrix is made up of various ECM molecules and cells loosely intermingling, whereas the basement membrane is composed of sheets of ECM molecules. The ECM molecules are mostly made up of various proteins, proteoglycans, and hyaluronan. The cells present in the connective tissue secrete ECM molecules and express receptors for attachment to them to help support and allow for growth and proliferation. ECM molecules are also particularly important in development, cell migration, tissue homeostasis, and even tumor invasion [15].

Integrins are the receptors on cell surfaces that are responsible for recognition of ECM and subsequent cellular response. They are heterodimeric receptors, divided into two functional subunits, α and β [17, 18]. Since ECM molecules have different chemical

compositions and interact with each other to form specific structural patterns, integrins respond to their bound ECM's as a combination of the two subunits based on chemical as well as physical cues [14 - 17]. During development, neurons express a large number of integrin receptors to help coordinate successful neural networks, but reduce in number in the adult brain [18]. Developing neurons, therefore, have the ability to grow on multiple different ECM proteins based on their characteristic integrin receptors present. During cell outgrowth, the leading end of the neuron is called the growth cone. It is an amoeboid structure with filopodia outgrowths that respond to extracellular cues in an attempt to reach a target cell to create a synapse [19, 20]. The growth cones of neurons have a large number of integrins that can either cause axon growth or inhibition based on the response to environmental factors. When a growth cone is exposed to a gradient of chemical cues in its environment, the filopodia protrude as a response to polymerization of actin and are exposed to different concentrations of the chemical cues based on location. The filopodia that are exposed to a higher concentration of the chemical cue will have a higher number of integrin binding than those exposed to less concentrated cues. Based on secondary messengers, the growth cone then polarized in response to the chemical cues, leading to the contraction of the cell and the depolymerization at the lagging end of the cell [20 - 22]. Therefore, if an ECM protein that attracts neurons is presented to a neuronal growth cone, the integrins will bind to the protein and cause the axon to grow toward the higher concentration of the protein [19]. Table 1.2 lists integrins present in the human body and their corresponding ligands.

Table 1.1 Ligand-binding specificities of human integrins [26]

Integrins	Ligands
α1β1	Laminin, collagen
α2β1	Laminin, collagen, thrombospondin, E-cadherin, tenascin
α3β1	Laminin, thrombospondin, uPAR
α4β1	Thrombospondin, MAdCAM-1, VCAM-1, fibronectin, osteopontin, ADAM, ICAM-4
α5β1	Fibronectin, osteopontin, fibrillin, thrombospondin, ADAM, COMP, L1
α6β1	Laminin, thrombospondin, ADAM, Cyr61
α7β1	Laminin
α8β1	Tenascin, fibronectin, osteopontin, vitronectin, LAP-TGF-β, nephronectin
α9β1	Tenascin, VCAM-1, osteopontin, uPAR, plasmin, angiostatin, ADAM [25], VEGF-C, VEGF-D [26]
α10β1	Laminin, collagen
α11β1	Collagen
αVβ1	LAP-TGF-β, fibronectin, osteopontin, L1
αLβ2	ICAM, ICAM-4
αMβ2	ICAM, iC3b, factor X, fibrinogen, ICAM-4, heparin
αXβ2	ICAM, iC3b, fibrinogen, ICAM-4, heparin, collagen [27]
αDβ2	ICAM, VCAM-1, fibrinogen, fibronectin, vitronectin, Cyr61, plasminogen
αIIbβ3	Fibrinogen, thrombospondin,, fibronectin, vitronectin, vWF, Cyr61, ICAM-4, L1, CD40 ligand [28]
αVβ3	Fibrinogen, vitronectin, vWF, thrombospondin, fibrillin, tenascin, PECAM-1, fibronectin, osteopontin, BSP, MFG-E8, ADAM-15, COMP, Cyr61, ICAM-4, MMP, FGF-2 [29], uPA [30], uPAR [31], L1, angiostatin [32], plasmin [33], cardiotoxin [34], LAP-TGF-β, Del-1
α6β4	Laminin
αVβ5	Osteopontin, BSP, vitronectin, CCN3 [35], LAP-TGF-β
αVβ6	LAP-TGF-β, fibronectin, osteopontin, ADAM
α4β7	MAdCAM-1, VCAM-1, fibronectin, osteopontin
αEβ7	E-cadherin
αVβ8	LAP-TGF-β

The brain is a highly organized network that controls the function of the body. Cell composition within the brain includes neural stem cells, neurons, astrocytes, oligodendrocytes, microglia, and ependymal cells [23, 24]. The neurons are the cells responsible for action potentials, the transmission of signal that leads to the functions of

the nervous system [25]. Cortical neurons are the neurons that are present in the cerebral cortex. The cerebrum is the large section of the brain that is seen as the majority of the external brain. The physical divisions based on location are the frontal lobes, the parietal lobes, the temporal lobes, and the occipital lobes. These divisions are associated with the bone that overlays them and are mostly associated with the functions that they coordinate. The cerebrum is also divided into two hemispheres, the left and the right. These two halves are connected mainly by the corpus callosum, which is a dense area of neurons that gather and coordinate the exchange of information between the hemispheres. The functional separations of the cerebrum include the cerebral cortex, the basal ganglia, and the limbic system [28].

The cerebral cortex is the few millimeter-outermost layer of the cerebrum that coordinates the higher brain functions including perception and movement. Each area of the cerebrum has it's own cortex function. The frontal lobe's cortex is divided into the primary motor cortex, motor association area, and prefrontal association area, which gather information from other areas of the brain associated with skeletal muscle movement and coordinate them for transmission to the muscles [26 – 28, 30]. Damage to or loss of a section of this area of the brain would lead to a loss of function of the associated skeletal muscles [29]. Since the cerebrum has a characteristic known as cerebral lateralization, meaning each hemisphere controls function of the opposite side of the body, a loss of part of the left sided frontal cerebral cortex would lead to paralysis of part of the right side of the body, and vice versa. The parietal lobe's cortex is divided into the primary somatic sensory cortex and sensory associated area. These work similarly to the frontal cortex except they receive the sensory input from the rest of the body and coordinate them into the brain's understanding of its environment [33, 34]. Sensation coordinated in this area of the brain includes that of the skin, the musculoskeletal system,

the taste buds, and the viscera, which is a term for the soft, internal organs in the abdomen, such as the intestines [31, 32]. Damage to or loss of this area of the brain leads to a lack of sensation from these areas of the brain listed. The occipital lobe cortex includes the sensory region of the brain associated with vision. Damage to or loss of part of this area of the brain would lead to partial or total blindness or any other abnormal visual perception [35]. The temporal lobe, located near the ears, contains the centers for hearing sensation and coordination. Similar to the visual cortex, loss of auditory cortex function would lead to abnormal auditory perception, such as deafness. Additionally, the olfactory cortex and the gustatory cortex are located within the brain and coordinate the smell and taste sensations, respectively. Again, loss of these areas would lead to lack of proper taste and smell perception, respectively. The association areas in each of these sections of the cortex are present to coordinate information between each other to allow for a smooth, voluntary perception and function [36].

The ECM proteins in the brain are composed mostly of Collagen, Laminin, Fibronectin, Vitronectin, and Tenascin [14, 15, 17]. Table 1.2 gives a graphical representation of the proteins listed along with their general structure, the integrin receptors that bind them, the neuronal types that are associated with these integrins, and the function induced by the proteins. The proteins used for this study are Laminin, Fibronectin, and Vitronectin.

Table 1.2 ECM proteins present in the brain with integrin receptors, affected neuronal types, and induced functions

ECM molecule	Integrin receptors	Neuronal type	Function
Collagen (protomer of 3 α chains)	$\alpha_1\beta_1$.	Rat sympathetic RGCs	Neurite outgrowth
	$\alpha_2\beta_1$.	DRG	Adhesion and neurite outgrowth
	$\alpha_1\beta_8$.	Motor, DRG	Neurite outgrowth
	(DDR1)	Cerebellar granule neurons	Neurite outgrowth
Laminin (trimer, αβγ chains)	$\alpha_1\beta_1$, $\alpha_1\beta_8$	DRG	Neurite outgrowth
	$\alpha_1\beta_1$, $\alpha_3\beta_1$	PC12, DRG, Cortical	Neurite outgrowth; migration
	$\alpha_1\beta_1$, $\alpha_4\beta_1$	Neural crest	Cell adhesion
	$\alpha_6\beta_1$	Retinal, Olfactory; Ciliary ganglion	Neurite outgrowth and migration
	$\alpha_3\beta_1$, $\alpha_7\beta_1$	Cortical	Neuritogenesis
	$\alpha_3\beta_1$, $\alpha_6\beta_1$, $\alpha_7\beta_1$	Adult DRG	Adhesion and neurite outgrowth
	$\alpha_3\beta_1$, $\alpha_6\beta_1$	Retinal, Hippocampal, Thalamic, Cortical	Adhesion and neurite outgrowth
Tenascin (hexbrachion, 190–300 kDa subunits) TN-C, TN-R, TN-W, TN-X, TN-Y	$\alpha_8\beta_1$	Motor, DRG	Neuritogeneis and neurite outgrowth
	$\alpha_7\beta_1$	cerebellar granule	Neurite outgrowth
	$\alpha_9\beta_1$	PC12, Adult DRG	Neurite outgrowth and regeneration
	(contactin)	Hippocampal	Neurite outgrowth
Fibronectin (~440 kDa dimer)	$\alpha_4\beta_1$	Chick DRG and sympathetic; Mouse retinal ganglion	Neurite outgrowth
	$\alpha_5\beta_1$	Cortical; Striatal progenitor cells	Neuronal differentiation and migration
	$\alpha_8\beta_1$	Chick DRG; Tectal	Adhesion, neurite outgrowth and migration
	$\alpha_v\beta_1$; $\alpha_v\beta_3$, $\alpha_v\beta_5$	Neural crest	Adhesion and migration
Vitronectin (75 kDa monomer)	$\alpha_v\beta_5$	Retinal; Cerebellar granule	Neurite outgrowth

1.4 Cancer

Cancer is a general term used in medicine to describe an uncontrolled growth of cells. In general, healthy cells multiply when they are required and die, i.e. apoptosis, when they are not required. These cells can, however, mutate in certain ways that affect these processes. A mutation is a change in a cell's genes that may or may not be harmful. Cancerous cells multiply and become large, clustered tumors that require abnormally large amounts of energy, blood, and oxygen to survive. The brain automatically accommodates to the requirements of these clusters, causing a deficiency of energy, blood, and oxygen to the surrounding healthy tissue and causing a list of physiological problems to the affected patient [39].

If a mutation occurs in one of the following three genes, cancerous growth may occur: oncogenes, tumor suppressor genes, and DNA repair genes [37, 40]. Oncogenes signal cells to multiply when necessary, such as post-injury or damage. In normal instances, the signals created by these genes are suppressed until an appropriate time. If oncogenes malfunction or are not present, the cells are continually signaled to multiply and a tumor may arise. Tumor suppressor genes are part of a healthy cell's natural defense against cancerous growth. These genes work specifically to stop any abnormal growth of cells, but can also mutate causing the ability for a cell to grow uncontrollably. The third type of gene that may cause cancerous growth if malfunctioning is the DNA repair gene. This gene mutation is the last mutational barrier a cell has to pass to become cancerous because these genes work to repair any mutations in any other genes when a cell is formed. If a mutation occurs in either an oncogene or a tumor suppressor gene, the DNA repair gene will usually correct the issue. However, if a combination of multiple gene mutations occurs, a cell can begin to multiply uncontrollably and become cancerous. Typically though, there are many fail-safes within a cell that recognize

mutation and either correct them or signal death of the cell. Additionally, if a cell does mutate and does not signal its own death, the body's immune system will generally recognize it as a foreign cell and will eliminate it. Due to the large amount of self-defense the body has associated with suppressing uncontrolled cell growth, cancerous growth is relatively rare [39 – 43].

Cancer in the brain is classified as benign or malignant and further classified based on the area of the brain affected. The following are the types of brain cancers generally seen: gliomas (further divided into astrocytomas, brain stem gliomas, optic nerve gliomas, and oligodendrogliomas), metastatic tumors, meningiomas, schwannomas, pituitary tumors, medulloblastomas, craniopharyngiomas, and pineal region tumors.

Glioblastoma Multiforme (GBM) is a one of the most invasive and deadly types of glioma currently known [41]. They account for approximately 15% of all brain tumors and 50% of gliomas. In two years after diagnosis, the survival rate is 3.3% and 1.2% at three years [43 – 46]. A unique characteristic of GBM is the fact that it grows by migrating outward from the tumor into surrounding healthy tissue [42, 47]. This fact contributes to the difficulty involved with treating this type of cancer. Surgical tumor removal, chemotherapy, and radiation therapy are all localized treatments that do not affect the outgrowths of cancer cells. Treatment of surrounding brain tissue can lead to healthy brain tissue loss, which would lead to the large number of problems outlined in 1.3, depending on the location. Tumor cell migration is dependent on the ECM molecules present in its environment as well as the cells it comes in contact with, so studying the interaction between tumor cells and their environmental factors is critical for better understanding of tumor growth and possible treatments.

1.5 Current research

Since GBM growth and penetration into healthy brain tissue is so highly dependent on the composition of ECM molecules surrounding it, it would be logical to obtain an in-depth understanding of the interactions involved. Experiments have been performed in the past involving exposure of GBM cells to various proteins and chemoattractants by either 2-D or 3-D assays [48, 49]. The goal of these experiments is to simulate the microenvironments that would be presented to these cells *in vivo*. One such device involves using a 3-D Boyden chamber assay made from a gel including ECM proteins [48]. They simulated the basal lamina with proteins and included a gradient of chemoattractant molecules throughout the small pores of the chamber. With this experiment, they obtain data regarding growth patterns when the cells are exposed to that particular set of conditions.

Another type of cell migration study involves growing cells on a platform adsorbed with alternating stripes of proteins [50]. The platform was created by adhering a stripe-containing matrix to the surface of the petri dish and either injecting one protein and filling the other into alternating stripes, or with vacuum assistance. Once the alternating protein stripes were adhered to the surface, cells were allowed to grow and were later quantified based on growth length. The main limitations of this experimental model when considering cell migration preference when exposed to multiple proteins include the inability to test more than two proteins at once and the fact that results are based solely on cell migration length. If a cell line were being tested for migration preference to multiple proteins, an ideal experiment would expose individual cells to all proteins in question before allowing them to grow, allowing the highest concentration of integrin-ligand binding to determine growth direction. In the case of GBM cells,

knowledge of migration preference could lead to better understanding of the outgrowth patterns into healthy brain tissue.

1.6 Objectives

The objectives of this project are to create a microfluidic device and model that will allow for a better understanding of cell-ECM interaction and characterize cells based on ECM migration preference. Specific aims include:

1. Design a microfluidic device and model that will provide an unbiased microenvironment that can allow for testing of cell migration preference to multiple ECM proteins.
2. Characterize GBM cells based on migration preference to common ECM proteins present in the brain.

Chapter 2

Microfluidic Device

2.1 Design of mask for soft lithography

The mask used during device fabrication held the designed microchannel system pattern. The mask was used to transfer the design to the master silicon wafer with photoresist, where PDMS devices could be made. AutoCAD was used to design the specific microchannel and reservoir dimensions of the mask and the fabrication from Mylar took place at an outside company. The device consisted of a large cell-seeding reservoir with two identical microchannel systems on either end. Each microchannel system consists of a 15mm wide, 150mm long microchannel that leads to a 3-way microchannel cross, each separated channel being 10mm wide and 5mm long. These microchannels lead to 2.5mm radius reservoirs for protein loading. The entire device was a single layer process with height 100mm. Figure 2.1 shows a schematic of the device design specifications.

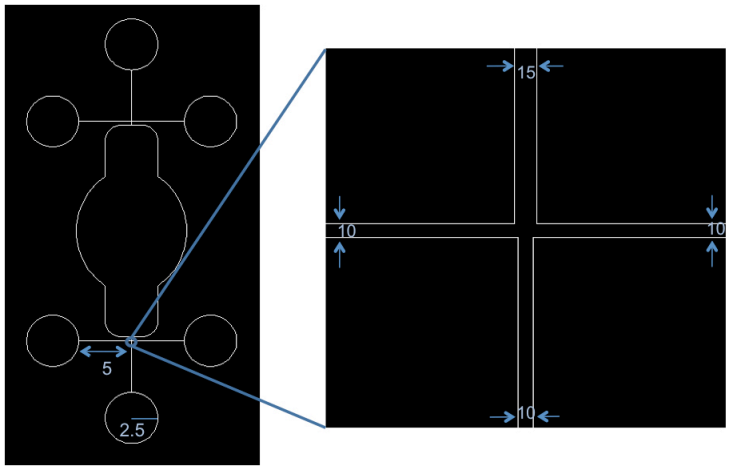

Figure 2.1 Schematic representation of device. Units for image containing entire image are in mm, units for enhanced microchannel cross are in mm.

2.2 Creation of silicon mold via soft lithography

All steps outlined in this section were performed in the Nanofabrication building at The University of Texas at Arlington. A 4-inch silicone water (Wafer world) was used along with photoresist SU-8 50 (MicroChem), SU-8 developer (MicroChem), a Spin coater, a Backside aligner, hot plates, acetone, and isopropyl alcohol. As a pretreatment step, the silicon wafer was cleaned with Acetone solvent followed by DI water (18.2 MΩ). The wafer is then dehydrated at 200 °C for 10 minutes on a hot plate to remove all moisture. To spin coat the photoresist, approximately 1 mL of resist per inch of wafer was added. The spin coater was increased in speed to ensure even coating at 100mm height. Initially it was increased to 500 rpm at 100 rpm/sec for 10 seconds, then increased to 1000 rpm at 300 rpm/sec for 30 seconds. The photoresist is then baked for 10 minutes at 65 °C then 30 minutes at 95 °C to ensure the solvent is evaporated and the resist film is dense. The photoresist is then cross linked when exposed to UV light (350-400 nm) in the specific pattern of the device. The exposure energy used was between 300 mJ/cm^2 – 550 mJ/cm^2. The UV was exposed to the wafer with mask for two consecutive 14-second intervals. The wafer was then heated in two steps to selectively cross-link the exposed regions and minimize damage to the pattern. It was first heated at 65 °C for 1 minute, then heated at 95 °C for 10 minutes. The wafer is then washed with SU-8 developer for 10 minutes to remove all photoresist that did not cross-link, which was not exposed to the UV. In the final step, the wafer is hard baked at 200 °C on a hot plate for 30 minutes to achieve maximum photoresist precision.

2.3 Polydimethylsiloxane (PDMS) microfluidic device fabrication

PDMS polymer was prepared for device fabrication by mixing polymer : curing agent in ratio of 10 : 1 respectively. The polymer mixture was then placed in a vacuum

dessicator at 20 in Hg for 45 minutes. When all air bubbles had been removed from the mixture, it was poured onto the silicon wafer mold, which had been placed in aluminum foil to avoid polymer leakage. The wafer with polymer was then placed on a hot plate at 150 °C for 5 minutes. Once the polymer had cured, the wafer was moved to a hot plate at 70 °C to allow for cutting of the device away from the silicon wafer. The wafer was placed on a 70 °C hot plate instead of the workbench to avoid cooling the wafer too quickly, which would lead to cracking. PDMS devices were created at approximately 4 mm in height. Once the device was cut to appropriate size, tissue biopsy punches were used to remove PDMS in reservoirs to allow for addition of cells and media. A 4mm biopsy punch was used to create the reservoirs at the ends of the microchannels as well as in the cell seeding area. Care was taken to ensure that the PDMS was punched out of the cell seeding area as close to the opening microchannel as possible to reduce culture time. The center of the device, which was used for medium change, was punched out with a 8mm biopsy punch. All punches in the center cell seeding area were connected.

The completed devices were then cleaned and sterilized. To begin cleaning, debris was removed using clear tape. Before sterilization, the devices were inspected carefully to ensure removal of all debris. The devices were then immersed in 70% ethanol and placed in a bio-safety cabinet for 25 minutes. After sterilization, the devices were removed from ethanol and placed in sterile DI water (18.2 MΩ) three times for 10 minutes each. After allowing to dry, the devices were ready for use. Figure 2.2 shows a picture of a device with biopsy punches used.

Figure 2.2 Punched device ready for cleaning and use in experimentation.

2.4 Assembly of device and setup of microenvironment

In the preliminary stages of this study, laminar flow of soluble proteins from the microchannels was applied directly to cells in the microchannels but the applied stress caused apoptosis and detachment from the surface. Studies performed in the past involving cells and laminar flow have mostly demonstrated how cells are affected by the high shear stress caused by the laminar flow, which can be applied to certain cells in a flowing environment such as blood vessels [66]. The technique was then developed to incorporate the PDITC protein immobilization treatment on the glass used to adsorb the proteins.

Coverglass cut to fit in a 60mm petri dish was treated with plasma for 30 minutes. It was placed in glass 60mm petri dishes and was incubated with a 2% APTES (3-Triethoxysilylpropylamine, Sigma) in 100% ethanol solution at room temperature. After 30 minutes, the APTES solution was removed, and the coverglass was washed with 100% ethanol 3 times and with DI water 3 times. A PDITC (p-Phenylene

diisothiocyanate, Sigma) solution was prepared by adding 0.002g of PDITC into the mixture of 9ml DMSO (dimethyl sulfoxide, Sigma) and 1ml pyridine (Sigma). This solution was applied to the APTES treated coverglass and was incubated at 55°C for 5 hours. After 5 hours, the PDITC solution was removed, and the coverglass was washed with 100% IPA (isopropyl alcohol) 3 times. It was then transferred into a bio-safety cabinet, washed with sterilized DI water 3 times and allowed to dry under sterilized bio-safety cabinet. The cleaned four-way microchannel device was placed in plasma treatment for 30 minutes and placed on top of the activated coverglass to ensure secure bonding between glass and device. Sterilized 1xPBS was then filled into the assembled devices until ready for use.

To begin the laminar flow of proteins, the 1xPBS was removed from the devices including cell seeding area and reservoir of each microchannel. First, the cell seeding area was filled with 300 μl of 1xPBS. Each protein-designated reservoir was initially filled with 3 μl of assigned protein solution (e.g., fluorescently tagged BSA or Laminin) at 100 μg/ml, then filled with additional 55 μl of 1xPBS. The devices were then left in a 37^{o}C incubator for 4 hours. Washing the devices after the laminar flow of the protein was critical to avoid the leakage of the proteins into other microchannels. First, all 1xPBS was removed from the cell seeding areas. Then all solution was removed from the protein reservoirs. Next, 58 μl of 1xPBS was added into each of the protein reservoirs. Finally, 300 μl of 1xPBS was added into the cell seeding area and the devices were left for 10 minutes. The order of removing and adding fresh 1xPBS was repeated for 2 more times to completely remove the unbound proteins from the microchannels. After washing, the device was filled with cell culture medium until cells were seeded. To visualize the immobilized proteins on the microchannels using a laminar flow, the protein was

fluorescently tagged using a protein fluorescent tagging kit (Pierce). Figure 2.3 shows a schematic representation of the process for creating the microchannel environment.

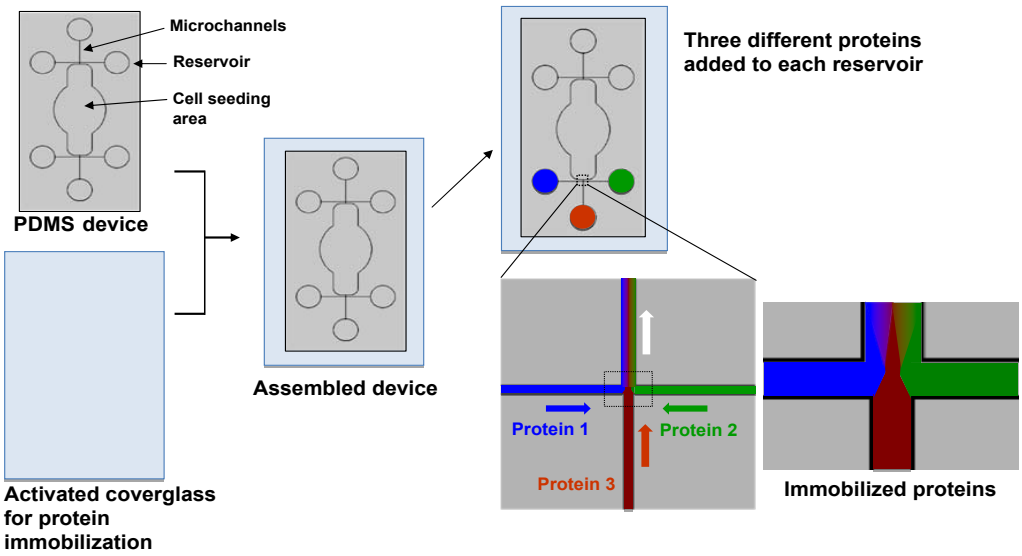

Figure 2.3 Schematic representation of the device setup and protein immobilization.

As seen in figure 2.3, the PDMS device with pattern was cut to fit onto an activated coverglass. Before assembly, the coverglass was already treated with PDITC to allow for protein immobilization. Once the PDMS device was attached to the coverglass, the three different proteins were filled into the three reservoirs separately, as depicted in the image as the three different colors. During the process of immobilization, the soluble proteins flow through the channels in a laminar fashion and deposit into the cell seeding area. After washing, they are immobilized, as seen in the bottom right corner of figure 2.3, in a manner in which the proteins are mixed prior to the microchannel cross and separate into their own channels as they near the cross.

Figure 2.4 shows the device before, during, and after simultaneous flow of two different fluorescently labeled BSA proteins.

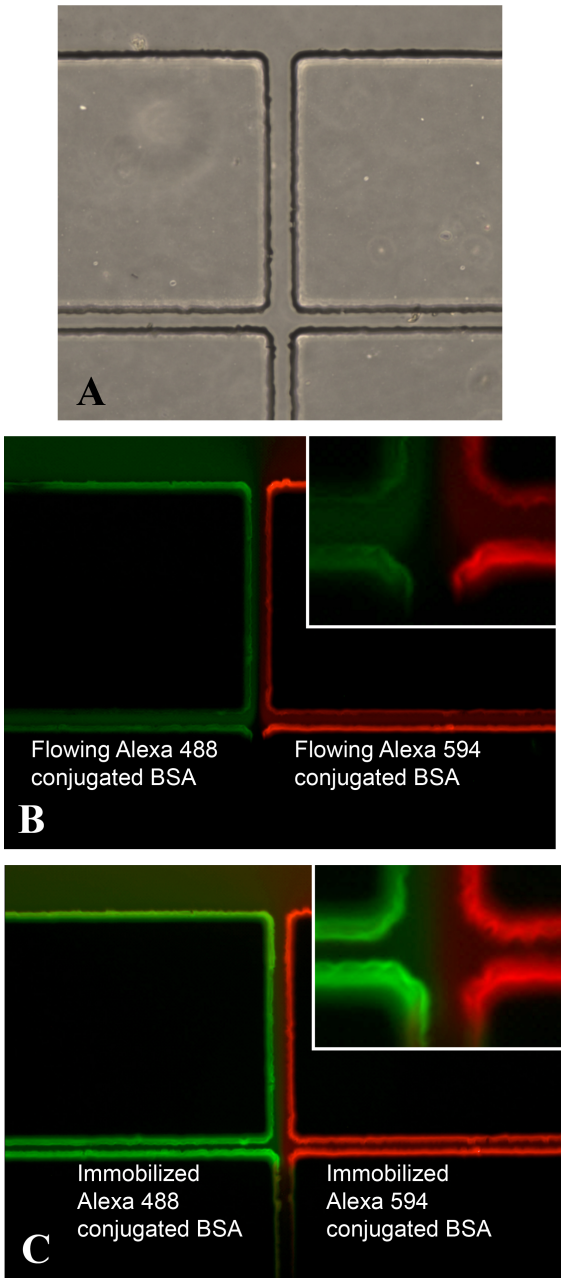

Figure 2.4 Images of a device before, during, and after flow of fluorescent BSA.

A) An image of the device at the microchannel cross at 10X magnification. B) The flowing of the Alexa conjugated BSA at 488 and 594 nm fluorescence from the left and right channels respectively. The laminar flow pattern in apparent, as magnified in the upper right corner. C) After allowing the proper time for flow, the device was cleaned properly and imaged again. The Alexa 488 and 594-conjugated BSA were immobilized onto the PDMS surface, as magnified in the upper right corner.

For a better visualization of the immobilization pattern of the protein onto its specific lane, Figure 2.4 shows the immobilization of Laminin onto one channel and no proteins immobilized onto the other channels. This figure also shows a device that was exposed to the same flow conditions with the same protein with the only exception being the lack of the PDITC treatment on the glass surface.

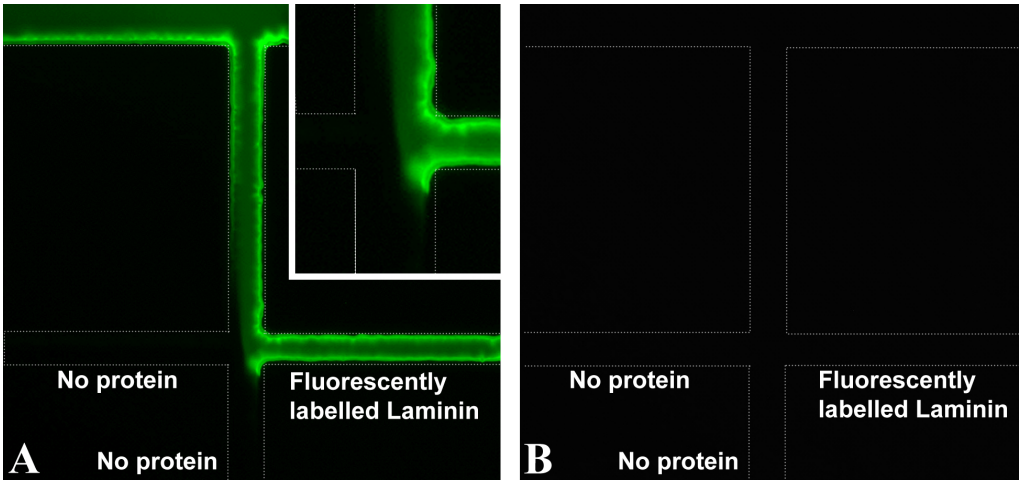

Figure 2.5 Fluorescently labeled Laminin immobilized onto one channel. Dashed lines represent microchannel walls. A) On PDITC treated glass, Laminin was immobilized onto one lane to better visualize the immobilization pattern. B) The same experiment was conducted in this image with the exception of the PDITC glass treatment procedure.

2.5 Results and conclusions

The device designed for this experiment allowed for the laminar, side-by-side flow of three different media into the cell seeding area. Once three different soluble proteins were placed into each of the three reservoirs, they flowed through the microchannels and mixed as they approached the cell seeding area, shown in Figure 2.3B. Once the adsorption had occurred and the device was washed, cells were seeded and allowed to grow. The microchannel leading to the cell seeding area showed a clearly mixed adsorption pattern closer to the cell seeding area and the protein adsorption separated closer to the microchannel cross. This allowed for each individual cell to be exposed to all proteins present in the device in the mixed area, then as they separated, the cells grew toward the protein that promoted growth the most. The magnification in Figure 2.3C shows the clear separation of the adsorbed proteins at the microchannel cross. For further understanding of the adsorption pattern, Figure 2.4A shows how the protein adsorbed from the flow of one channel adsorbs homogenously onto the microchannel leading to the cell seeding area but separates and leads only into the microchannel where it came from. This pattern of protein adsorption on activated glass perfectly allows for a totally unbiased cell migration preference study.

Figure 2.4B shows the same experiment performed in figure 2.4A except with the exception of using PDITC treated glass, demonstrating clearly that laminin could not adsorb to the surface. After washing the inactivated glass, all laminin was washed away and the fluorescent image was blank. The white dotted lines indicate where the walls of the channels are. These images make very clear the need for both PDITC-treated, activated glass and the use of protein laminar flow for the procedure to properly work. With these preliminary images taken, it would be logical for a cell from the above cell-

seeding area to grow and follow the laminin into its channel on the activated glass only, assuming laminin promoted the cell's growth.

Another interesting observation made from the fluorescent images taken is the fact that the microchannel walls are much brighter than the glass surface where the protein is immobilized. Due to it's chemical structure and properties, PDMS is known to swell in the presence of non-polar, organic solvents [1,5]. As noted in figure 1.1, PDITC is both non-polar and organic. Although the glass is treated with PDITC prior to adhesion to the PDMS device, the high shear forces involved with the immobilization process most likely causes some of the PDITC molecules to detach from the glass surface. Once detached, the PDITC molecules would be free to swell into the PDMS and allow for protein immobilization onto the PDMS surface as well. Since the fluorescent images taken are from a top-down manner, the bright PDMS walls are the accumulation of the 100μm height of the microchannel, whereas the width is only 10μm. Even if the microchannel walls (the PDMS) had less adsorbed protein than the glass surface, the 100μm stack would look more concentrated than the flat glass surface. Since the device visualized in figure 2.4B did not have any PDITC present, there was no fluorescence seen from the microchannel walls.

Chapter 3

Cortical Neuron Experimentation

3.1 Cortical neurons and proteins

Cortical neurons are the primary cell type in the cerebral cortex and are responsible for many higher functions of the brain such as voluntary movement and thought [52]. Laminin is a heterotrimeric proteins consisting of an α, β, and γ unit that is very substantially present in the cerebral cortex [53]. Laminin is well known to cause growth-promotion and regeneration of cortical axons as well as have a major role in the development of the brain [51 – 56, 59, 60]. As seen in Table 1.2, laminin binds to the following integrin couples on cortical neurons: $\alpha_1\beta_1$, $\alpha_3\beta_1$, $\alpha_6\beta_1$, and $\alpha_7\beta_1$. Aggrecan is a chondroitin sulfate proteoglycan (CSPG) that is present in the central nervous system and is known to inhibit neuronal axon growth [16, 57]. For example, aggrecan is released after a spinal cord injury and contributes to the glial scar that causes paralysis [57, 58].

3.2 Cell harvesting and culture

All procedures were conducted according to IACUC (Institutional Animal Care and Use Committee) approved protocols at the University of Texas at Arlington. Cortical neurons were isolated from embryonic 18-day rat embryos. The cortical brain tissues were dissected, cleaned, minced and enzymatically dissociated (0.125% trypsin in L-15 medium) for 20 minutes at 37^{o}C. Twenty minutes after, soybean trypsin inhibitor (SBTI, 1.5% (w/v), Worthington) was added and mechanically dissociated using a fire polished glass pipette. The dissociated cells were centrifuged and seeded into the cell seeding area (100,000 neurons per device). Cortical neurons were seeded into devices (n=4)

where laminin (10mg/ml) was adsorbed onto one microchannel and aggrecan (500μg/ml) was adsorbed onto the other two microchannels. Serum free cell culture medium (Neurobasal medium supplemented with B-27, invitrogen, and growth factors, BDNF and NT-3, 10 ng/ml, Peptrotech) was changed every 2-3 days until cortical axons preferentially outgrew toward the specific protein.

3.3 Experiments and Results

Cortical neurons were seeded into devices (n=4) where laminin (10mg/ml), a growth promoting protein, was adsorbed onto one microchannel and aggrecan (500μg/ml), a growth inhibiting protein, was adsorbed onto the other two microchannels. Serum free cell culture medium (Neurobasal medium supplemented with B-27, invitrogen, and growth factors, BDNF and NT-3, 10 ng/ml, Peptrotech) was changed every 2-3 days until cortical axons preferentially outgrew toward a protein. The cortical neurons were given sufficient time to allow for significant growth into the preferred channel. It became very evident that laminin was preferred over aggrecan in all experimental trials. Cells did, however, proliferate occasionally into the other two channels, but after short distances growth stopped and the axons only continued into the laminin channel. Figure 3.1 shows a montage of the fluorescent and bright field images superimposed onto one another of one device 8 days after cell seeding. In the upper right corner of the figure there is a magnification of the leading end of the neuronal axon on the laminin-coated microchannel. Due to the high intensity of fluorescence at the microchannel cross, the fluorescent image of the axons leading from the cell seeding area was difficult to visualize.

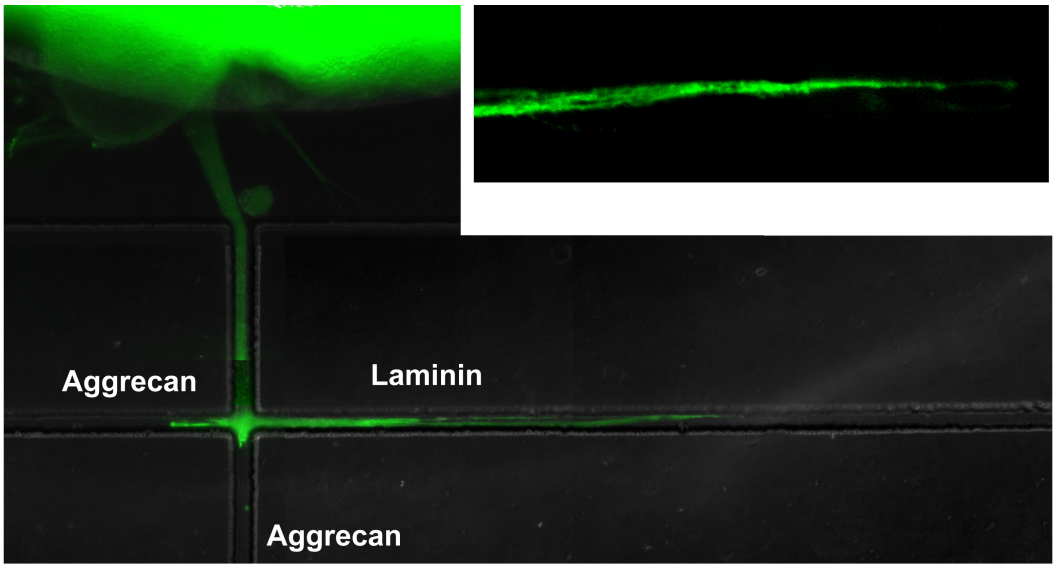

Figure 3.1 Cortical neurons experimental results in 10X fluorescence and bright field.

3.4 Conclusions

The experimental trials with cortical neurons served as a control for this device to prove if it worked as expected. Since it is well known that a neuronal axon would grow on laminin opposed to aggrecan if given the opportunity, we had an expected outcome that we ended up observing. In all cases, there was an obvious growth into the microchannel coated with laminin and almost no growth into the microchannels coated with aggrecan. As seen in Figure 3.1, there is a small amount of growth into one of the aggrecan-coated channels, but significantly less than that in the laminin-coated channel. Upon initial growth of the first axon into the microchannel, there was a clear growth toward laminin. As more axons grew into this microchannel, however, the laminin-coated microchannel became essentially full or crowded. When the availability to grow onto the laminin-coated channel was no longer an option, the axonal growth cones would attempt to grow on the aggrecan-coated microchannels and stop after a very short distance.

With the results from this experiment, it becomes apparent that the initial idea and goal for the device was possible. Initial fluorescence experiments, as seen in figures 2.3 and 2.4, prove that the proteins can immobilize in a desired pattern, while the cortical neuron control experiments, as seen in figure 3.1, proves that cells can preferentially grown on the device model. The final goal of use with the designed device is the ability to identify the preferential growth patterns of cells that do not already have a known list of integrins. As most of the cells that are normally present in the human body have been studied for their growth properties and patterns, use with this device would be mostly to confirm what is already widely understood. Instead, cells that do not have a vast amount of knowledge known about them would benefit from this experimental model, such as cancer cells.

Chapter 4

Glioblastoma Multiforme Experimentation

4.1 GBM and proteins

Glioblastoma multiforme (GBM) is the most deadly type of brain tumor and has very low survival rates [41]. Patients with GBM continually have recurrence of the tumor after surgical resection, chemotherapy, and radiation therapy due to the cancer's ability to migrate and infiltrate surrounding healthy brain tissue [42, 47, 61]. The mode of cell migration is similar to that of neuronal axons with growth cones. The GBM cells modify their cellular structure, including shape and rigidity, to allow for interaction with surrounding cells and ECM molecules. The cells polarize and extend actin-containing structures that interact with the surrounding microenvironment mainly with integrin receptors [61]. Once the cell has adhered to a particular ECM protein, for example, the intermolecular chemical reactions trigger the structural change of the cell, including contraction and movement. When comparing GBM cells to healthy brain cells, GBM over-expresses the integrins $\alpha_2\beta_1$, $\alpha_3\beta_1$, $\alpha_5\beta_1$, $\alpha V\beta_3$ [62]. These integrins have been shown to be directly involved with cell migration and proliferation as well as cancer cell invasion in the brain [62-64]. As seen in table 1.1, the major brain ECM components that these integrins bind to are as follows. Integrin $\alpha_2\beta_1$ binds to laminin and collagen, integrin $\alpha_3\beta_1$ binds to laminin, integrin $\alpha_5\beta_1$ binds to fibronectin, and integrin $\alpha V\beta_3$ binds to fibronectin, vitronectin, and tenascin [17]. Therefore, it would be logical that the GBM cells would have highly proliferative growth and migration within healthy brain tissue. The generally accepted procedure for identifying a cell's integrin composition is using an anti-integrin antibody assay [65]. Since multiple integrins can bind to the same proteins, exact migration patterns

cannot be fully characterized by investigating the integrin-composition of the cell alone. Since GBM is so deadly due to its migration patterns, having a comprehensive understanding of the migration habits of these cells may lead to new treatment technique.

4.2 Cell extraction and culture

Two different primary human-derived glioblastoma (hGBM) cells were obtained from consenting patients at the University of Texas Southwestern Medical Center (Dallas, TX, USA) with the approval of the Institutional Review Board. These two hGBM cells were collected from two different patients. First hGBM cells (133p, n=13) were stably transduced with a lentivirus expressing *m-cherry* fluorescent protein and were seeded on the cell seeding area of devices with laminin (10mg/ml) adsorbed onto one microchannel, fibronectin (10mg/ml) adsorbed onto another microchannel, and no protein adsorbed onto the third microchannel. Second hGBM cells (C419, n=5) were seeded on the cell seeding area of devices with laminin, fibronectin and vitronectin (10mg/ml). Serum free cell culture medium (DMEM/F-12 supplemented with B-27, and growth factors, mEGF and bFGF, 20ng/ml, Peptrotech) was changed every 2-3 days until hGBM cells preferentially migrated toward the specific protein. hGBM 133P cells were given 7 days to grow before fixation with 4% paraformaldahyde, and hGBM C419 cells were given 4 days to grow before fixation with 4% paraformaldahyde.

4.3 hGBM 133P experiments and results

Human glioblastoma multiforme cells (133P strain) were seeded onto devices with Laminin adsorbed onto one microchannel and Fibronectin adsorbed onto another microchannel to attempt to differentiate the cell's preference to these two proteins, since they are both highly involved with promoting GBM migration [62, 63]. Figures 4.3A and 4.3B

show two of the thirteen trials conducted with the same experimental setup. DAPI staining allowed for quantification of the number of cells that grew toward each protein. The total number of cells in each microchannel was recorded and averaged among all trials. Comparing the averages of these values showed no statistically significant difference between the protein preferences. Figure 4.2 shows graphical representation of the total average number of cells that proliferated into each of the respective channels from all combined trials with statistical significance represented. Table 4.1 shows the data from each of the individual thirteen experimental trials with hGBM 133P. From the Tukey simultaneous tests performed, the p-value for comparison between Laminin and Fibronectin was 0.5603, the p-value for comparison between Laminin and no protein was 0.0038, and the p-value for comparison between Fibronectin and no protein was 0.0509.

Table 4.1 Data from each experimental trial with hGBM 133P

Trial	Laminin (#)	Fibronectin (#)	No Protein (#)
1	47	48	2
2	45	19	2
3	11	8	0
4	27	29	1
5	4	14	0
6	19	11	1
7	1	6	0
8	6	2	0
9	7	5	0
10	8	4	0
11	22	3	0
12	4	0	0
13	13	3	0
Average	16.46153846	11.69230769	0.461538462
SD	15.15814074	13.56702261	0.776250026
SEM	4.204111822	3.762815053	0.215293021

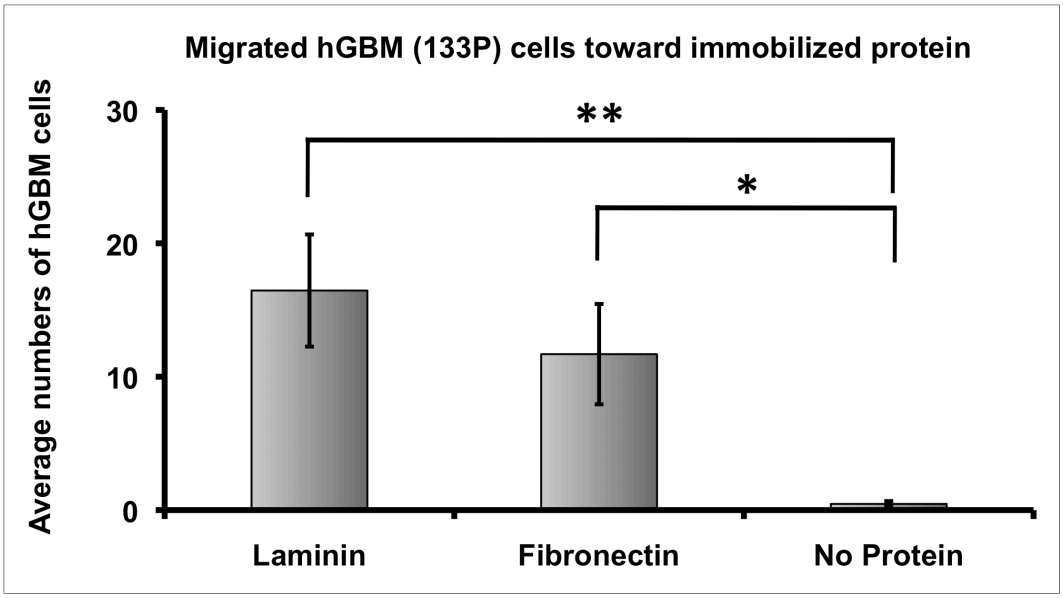

Figure 4.1 Averaged total number of hGBM (133P) cells migrated into channels with respective proteins from all trials.

To correct for possible irregularities between trials, leading to the large error, the data was normalized per device to represent the percent of cells that migrated into each microchannel from the total number in the device. These percentages were then averaged among all trials and compared for statistical significance. Figure 4.2 shows graphical representation of the average percent of cells that proliferated into each of the respective channels from all combined trials with statistical significance represented. Table 4.2 shows the normalized data from each of the individual thirteen experimental trials with hGBM 133P. From the Tukey simultaneous tests performed, the p-value for comparison between Laminin and Fibronectin was 0.0184, the p-value for comparison between Laminin and no protein was below 0.0000, and the p-value for comparison between Fibronectin and no protein was 0.0001.

Table 4.2 Normalized data from each experimental trial with hGBM 133P

Trial	Laminin (%)	Fibronectin (%)	No Protein (%)
1	48.45	49.48	2.06
2	68.18	28.79	3.03
3	57.89	42.11	0.00
4	47.37	50.88	1.75
5	22.22	77.78	0.00
6	61.29	35.48	3.23
7	14.29	85.71	0.00
8	75.00	25.00	0.00
9	58.33	41.67	0.00
10	66.67	33.33	0.00
11	88.00	12.00	0.00
12	100.00	0.00	0.00
13	81.25	18.75	0.00
Average	60.68821872	38.53698504	0.77479624
SD	24.12553784	24.07579133	1.262063881
SEM	6.691220287	6.677423087	0.350033541

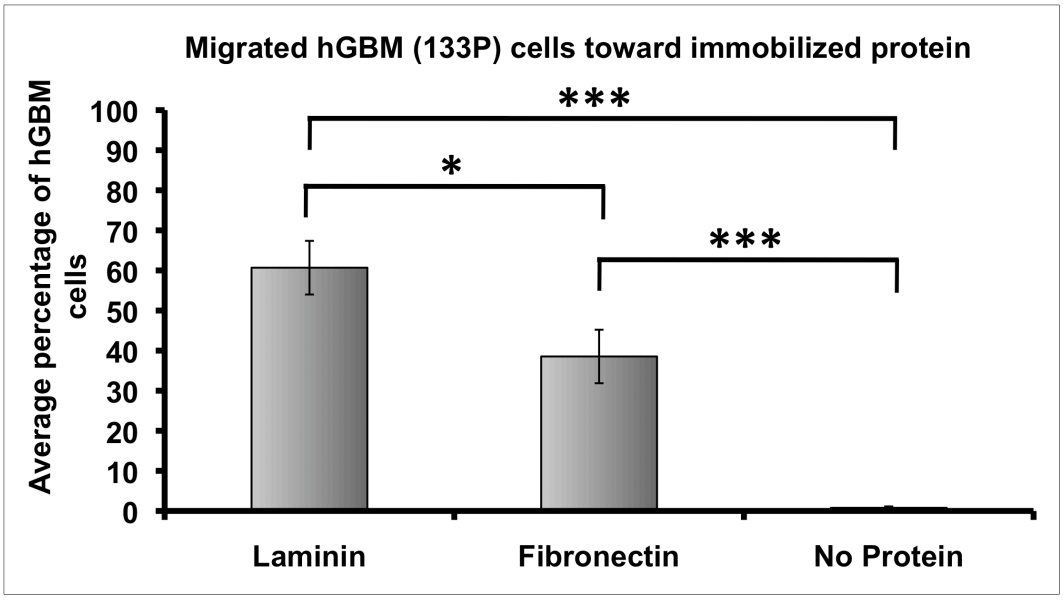

Figure 4.2 Averaged percent number of hGBM (133P) cells migrated into channels with respective proteins from all trials.

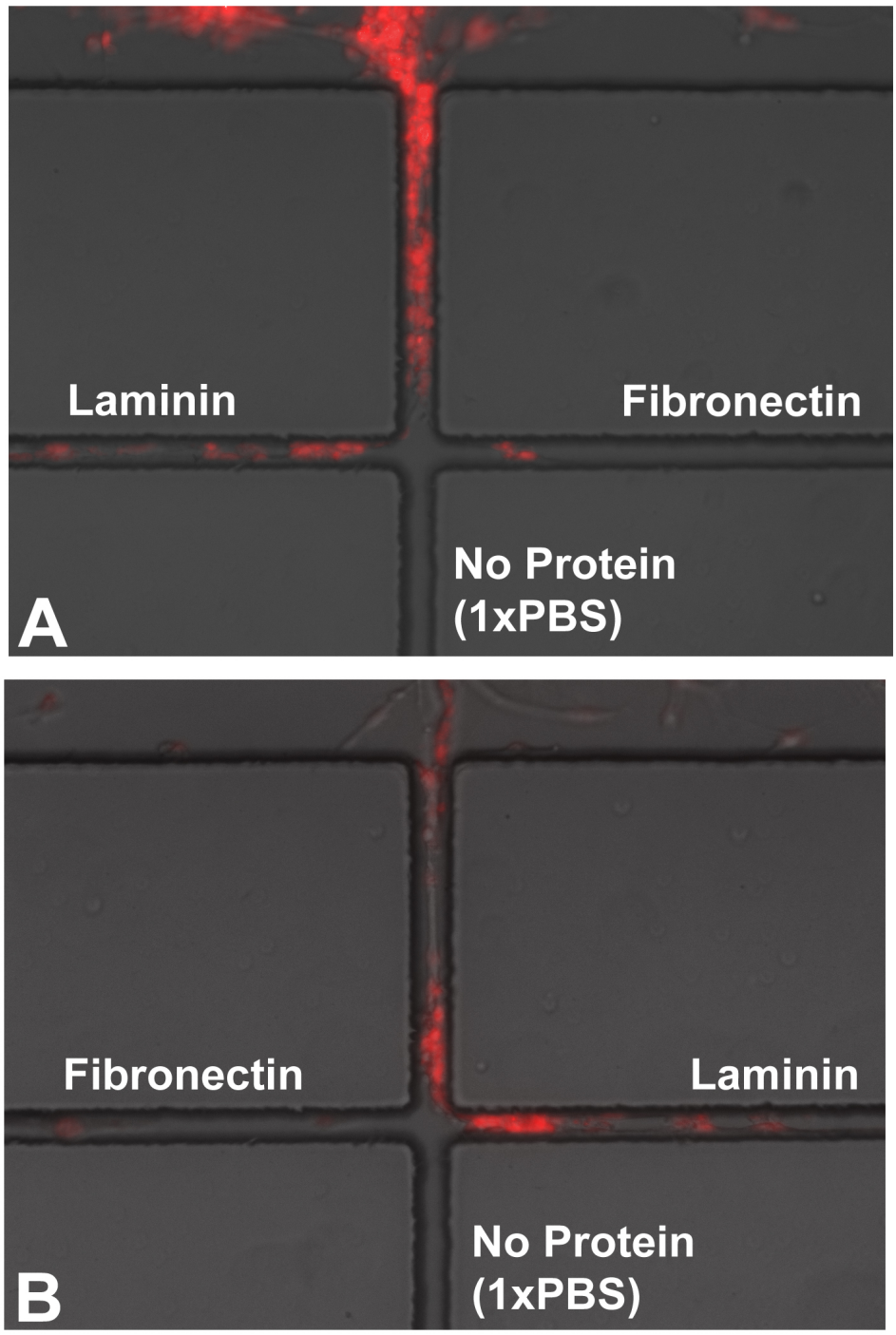

Figure 4.3 GBM (133P) fluorescent and bright field images with DAPI staining. A) Laminin was adsorbed onto the left channel and fibronectin was adsorbed onto the right

channel. 133P strain hGBM cells proliferated toward both proteins but showed slightly greater affinity towards laminin. B) Laminin was adsorbed onto the right channel and laminin was adsorbed onto the right channel. Experiment conducted similar to A.

4.4 hGBM C419 experiments and results

A second strain of human glioblastoma multiforme cells (C419 strain) was similarly tested for protein preference. In this experiment, however, the proteins Laminin, Fibronectin, and Vitronectin were all compared simultaneously. Each of these three proteins were adsorbed onto separate microchannels in different orders for each of the 5 trials. In all five trials, 100% of cells proliferated toward laminin. Figures 4.3A and 4.3B show two of the experiments performed. To disprove the possible hypothesis that cells were simply growing along a PDMS wall rather than according to protein preference, Figure 4.3C shows an experiment performed with C419 cells in which Laminin was adsorbed onto the center channel. 100% of cells, regardless of protein adsorption pattern, grew across the microchannel cross into the center lane. Figure 4.4 shows graphical representation of the average number of cells that proliferated into each of the respective channels from all combined trials with statistical significance represented. Table 4.2 shows the data from each of the individual five experimental trials with GBM C419. From the Tukey simultaneous tests performed, the p-value for comparison between Laminin and Fibronectin was below 0.0000, the p-value for comparison between Laminin and Vitronectin was below 0.0000, and the p-value for comparison between Fibronectin and Vitronectin was 1.0000.

Table 4.3 Data from each experimental trial with hGBM C419

Trial	Laminin (#)	Fibronectin (#)	Vitronectin (#)
1	4	0	0
2	8	0	0
3	5	0	0
4	6	0	0
5	4	0	0
Average	5.4	0	0
SD	1.673320053	0	0
SEM	0.464095481	0	0

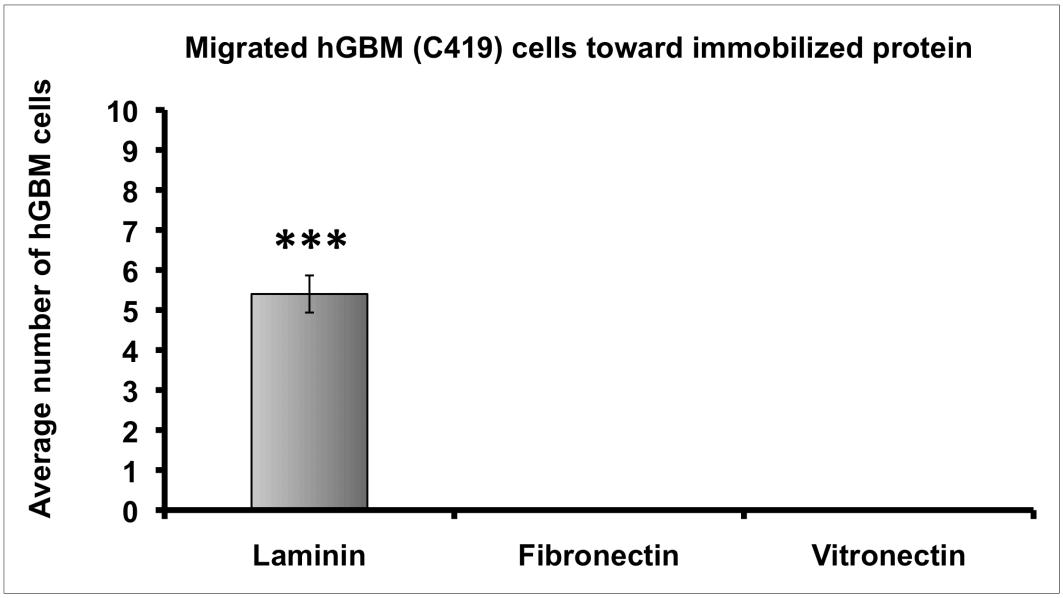

Figure 4.4 Averaged total number of hGBM (C419) cells migrated into channels with respective proteins from all trials.

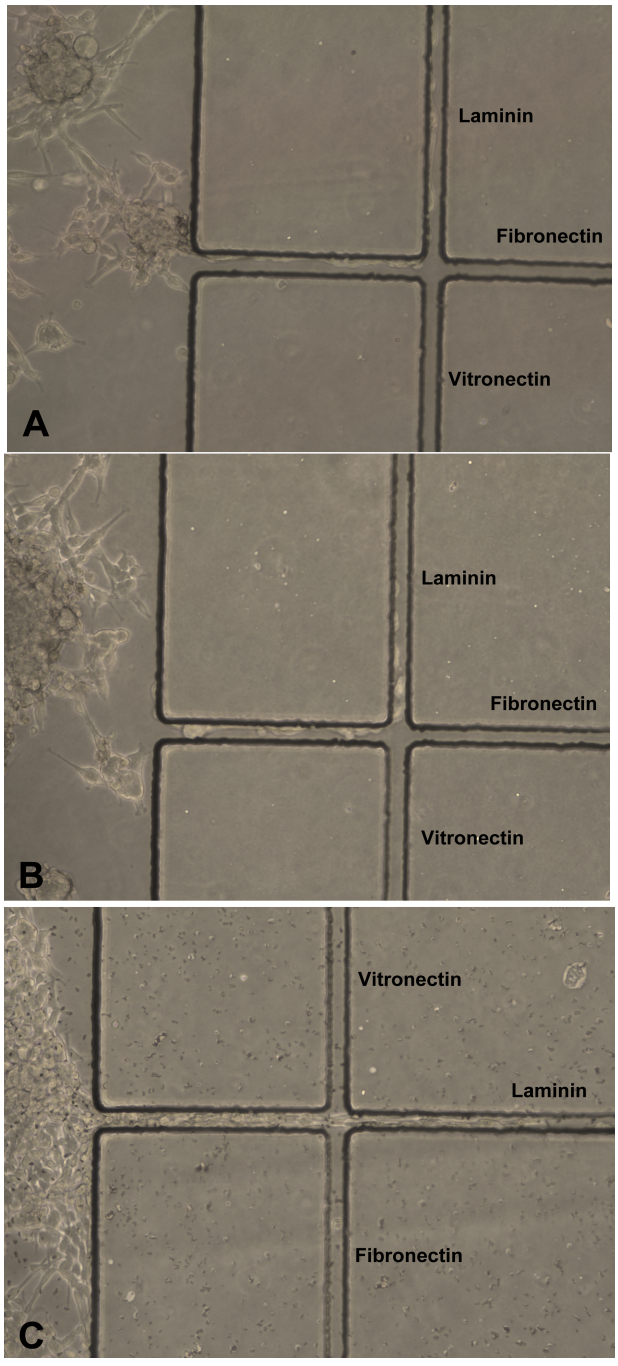

Figure 4.5 hGBM (C419) bright field images. A) Laminin was adsorbed onto the upper channel, fibronectin onto the middle channel, vitronectin onto the bottom channel. C419 hGBM cells showed 100% proliferation toward laminin. B) Same experimental setup as

in 4.5A with similar results. C) Vitronectin was adsorbed onto the upper channel, laminin onto the middle channel, and fibronectin onto the bottom channel. C419 hGBM cells showed 100% proliferation toward laminin.

4.5 Conclusions and discussion

From the initial 133P results based purely on number of cells migrated into microchannels, as seen in figure 4.1 and table 4.1, there was no statistically significant difference between Laminin and Fibronectin, but there was a difference between Laminin and no protein at above 99% confidence, and a difference between Fibronectin and no protein at above 95% confidence. As seen in the data from the individual trials, there was a large total cell number difference between some of the trials with some trials having total number of migrated cells above 80, where some are as low as 4 or 6. Although the number of cells seeded and the duration of culture time remained constant throughout, the difference was most likely due to the technique in preparation of the device itself. When the biopsy punch was used to create the reservoir for the cell seeding area, the distance between the reservoir edge and the microchannel opening directly had an impact on the number of cells that grew into the microchannels over the trial time. For the devices with a larger distance between the reservoir edge and microchannel opening, cell clusters formed further away from the microchannel upon initial cell seeding than those with shorter distances. Due to the gradient created by the flow of proteins from the microchannel into the cell seeding area, cell clusters that are further from the microchannel opening would be less affected by the proteins than those that are closer. Over the same period of time, the total number of cells migrated into the microchannels in all trials would be expected to be very different. This fact lead to the high error seen in the data and figure. As one way to improve the experimental design, a

technique would need to be designed to ensure a more consistent reservoir-to-microchannel distance in all devices. Given this method of statistical analysis, 133P strain of hGBM preferentially migrates toward either laminin or fibronectin over the channel with no protein adsorbed, but shows no preference to laminin over fibronectin or vice versa. Since the microchannel containing “no protein” simply had PDITC groups present on the glass surface, leaving the surface non-polar and hydrophobic, the preference of cells to grow on laminin and fibronectin over that microchannel is logical and expected.

To compensate for the difference in total number of migrated cells seen in the 133P experiments, the number of cells in each microchannel was taken as a percentage of the total migrated cells for each individual trial. Once all data from each trial had been converted to percentages, they were again averaged and tested for statistical difference. When using this technique, it was observed that there was a statistically significant difference between laminin and fibronectin at a confidence of above 95%, while there was a difference between laminin and no protein at a confidence of above 99.9% and between fibronectin and no protein at a confidence of above 99.9%. Therefore, given this method of statistical analysis, 133P strain of hGBM preferentially migrates toward laminin over fibronectin, and preferentially migrates toward both laminin and fibronectin over the microchannel with no protein adsorbed.

When considering the five trials with hGBM C419, it is observed that 100% of cells in every trial grew toward laminin over fibronectin or vitronectin. A concern at this point of experimentation was that cells were simply following a PDMS wall as they turned and were not actually making a protein preference decision. To counter this question, laminin was adsorbed to the center microchannel opposed to one of the side microchannels, as seen in figure 4.4C. As observed, the cells grew directly across the

microchannel cross into the middle microchannel containing laminin. This proves that the cells are truly growing toward the protein preference rather than being affected by the PDMS. All trials had relatively similar number of cells in the laminin microchannels, allowing for a small error. Unlike the 133P experiments, taking a percentage is not necessary since it can already be stated that there is statistical difference between laminin and fibronectin as well as laminin and vitronectin at a confidence over 99.9%. Since there were no cells in any of the fibronectin or vitronectin microchannels in any trial, the p-value of 1.0000 leads to a total lack of statistical difference. Therefore, given this method of statistical analysis, C419 strain of hGBM preferentially migrates strongly toward laminin over fibronectin or vitronectin. Although the percentage analysis of hGBM 133P showed significant difference between laminin and fibronectin as well, there were still a comparable number of cells in both microchannels in any given trial, whereas the C419 trials showed 100% cell growth toward laminin.

With the data from these two different hGBM experiments, it has become evident that different strains of hGBM have different characteristics, namely migration patterns. This leads to the conclusion that different hGBM strains in different patients have varying integrin compositions, resulting in the difference in migration preference. This would be important to know on a patient-by-patient basis to better understand the infiltration pattern of cancer cells into the healthy brain tissue. The leading cause of patient death due to hGBM is the inability to completely destroy the tumor cells without destroying too large of a section of brain. This is caused by the infiltration and migration of cells into healthy brain tissue leading away from the solid tumor mass. If a patient that is diagnosed with GBM presents to a oncologist and a biopsy of the tumor is acquired, protein migration preference could be determined. For example, if the patient's cells were to show 100% migration preference toward one particular protein similar to that of the trials conducted

with hGBM C419, knowledge could be acquired about the migration patterns of tumor cells away from the main solid tumor mass in their brain based on the protein composition of various areas of the brain. With simple anti-integrin antibody studies, the composition of integrins in a particular type of cell can be determined, but the overall interaction between these integrins when actually exposed to proteins would not be understood without actually performing this new test. Although cell migration within the brain is due to surrounding cells as well, interaction with ECM proteins is a major factor. The brain contains more than three proteins in its ECM, so several different trials would have to be conducted with different proteins in different arrangements on the three microchannels to get a true understanding of the migration preference in the brain as a whole.

A successful device has been demonstrated that can create a microenvironment that allows for exposure of individual cells to multiple proteins and determines migration preference toward these proteins when they separate into their respective microchannels. Given the two different strains of hGBM, experiments were conducted that gave insight regarding their protein preference to a select list of ECM proteins present in the brain. Research in the past has never been able to successfully expose individual cells to multiple proteins before quantitatively analyzing migration. This form of protein exposure is crucial when studying migration patterns of tumor cells for several reasons. When hGBM cells are present in a live human brain, they are exposed to multiple proteins simultaneously due to the vast complexity of the brain. Therefore testing of migration preference in any other manner would not be as effective. Additionally, the interaction of a cell with multiple proteins may change the migration patterns as compared to being exposed individually or with fewer proteins. For example, the trials conducted with hGBM 133P exposed the cells to laminin and fibronectin and a certain preference outcome was

observed. If these cells were exposed to laminin, fibronectin, and vitronectin, similar to that of the trials conducted with hGBM C419, a different preference outcome may be observed.

In general, this *in vitro* model is a positive step toward a better understanding of the processes involved with *in vivo* hGBM. The major limitations of this experimental model include the inconsistency of distance between the microchannel opening and the cell seeding reservoir edge created by biopsy punch and the fact that the device only allows for presentation of three proteins at once.

Chapter 5

Future Work

The brain ECM being much more complex than three proteins, a more complex version of this experimental model would be ideal to further understand the migration patterns of hGBM in the brain. If the original schematic design for the device were expanded to include five microchannels in which the five major brain ECM component proteins, as seen in table 1.2, could be added, the experiment could be conducted to demonstrate preference when cells are exposed to all these proteins simultaneously. The most difficult component of designing this experimental model was establishing the appropriate volume and concentration of protein to add to the microchannel reservoirs as well as the incubation time to most efficiently adsorb proteins to the microchannels. With five or more microchannels, as long as the same fluid mechanic properties applied including laminar flow, adsorbing the proteins in a similar pattern should be possible.

Since the PDITC on the glass surface immobilizes proteins by covalently bonding to their amino groups, this device model can be used for any protein and any cell combination as well as any other molecule that contains amino groups. This model will also prove useful for similar experimentation with other cancer types.

References

REFERENCE LIST:

[1] Michelsen, U. (2007). "Microfluidics in medical applications." Med Device Technol **18**(3): 12-14.

[2] Situma, C., M. Hashimoto, et al. (2006). "Merging microfluidics with microarray-based bioassays." Biomol Eng **23**(5): 213-231.

[3] Weibel, D. B. and G. M. Whitesides (2006). "Applications of microfluidics in chemical biology." Curr Opin Chem Biol **10**(6): 584-591.

[4] Dutse, S. W. and N. A. Yusof "Microfluidics-based lab-on-chip systems in DNA-based biosensing: an overview." Sensors (Basel) **11**(6): 5754-5768.

[5] Regehr, K. J., M. Domenech, et al. (2009). "Biological implications of polydimethylsiloxane-based microfluidic cell culture." Lab Chip **9**(15): 2132-2139.

[6] Dodge, A., E. Brunet, et al. (2006). "PDMS-based microfluidics for proteomic analysis." Analyst **131**(10): 1122-1128.

[7] Wong, I. and C. M. Ho (2009). "Surface molecular property modifications for poly(dimethylsiloxane) (PDMS) based microfluidic devices." Microfluid Nanofluidics **7**(3): 291-306.

[8] McDonald, J. C., D. C. Duffy, et al. (2000). "Fabrication of microfluidic systems in poly(dimethylsiloxane)." Electrophoresis **21**(1): 27-40.

[9] Guo, Z., R. A. Guilfoyle, et al. (1994). "Direct fluorescence analysis of genetic polymorphisms by hybridization with oligonucleotide arrays on glass supports." Nucleic Acids Res **22**(24): 5456-5465.

[10] Moller, R., A. Csaki, et al. (2000). "DNA probes on chip surfaces studied by scanning force microscopy using specific binding of colloidal gold." Nucleic Acids Res **28**(20): E91.

[11] Wan, Y., Y. T. Kim, et al. "Surface-immobilized aptamers for cancer cell isolation and microscopic cytology." Cancer Res **70**(22): 9371-9380.

[12] Gandhiraman, R. P., V. Gubala, et al. "Deposition of chemically reactive and repellent sites on biosensor chips for reduced non-specific binding." Colloids Surf B Biointerfaces **79**(1): 270-275.

[13] Dertinger, S. K., X. Jiang, et al. (2002). "Gradients of substrate-bound laminin orient axonal specification of neurons." Proc Natl Acad Sci U S A **99**(20): 12542-12547.

[14] Novak, U. and A. H. Kaye (2000). "Extracellular matrix and the brain: components and function." J Clin Neurosci **7**(4): 280-290.

[15] Ruoslahti, E. (1996). "Brain extracellular matrix." Glycobiology **6**(5): 489-492.

[16] Barros, C. S., S. J. Franco, et al. "Extracellular matrix: functions in the nervous system." Cold Spring Harb Perspect Biol **3**(1): a005108.

[17] Myers, J. P., M. Santiago-Medina, et al. "Regulation of axonal outgrowth and pathfinding by integrin-ECM interactions." Dev Neurobiol **71**(11): 901-923.

[18] Pinkstaff, J. K., J. Detterich, et al. (1999). "Integrin subunit gene expression is regionally differentiated in adult brain." J Neurosci **19**(5): 1541-1556.

[19] Estrada-Bernal, A., S. D. Sanford, et al. "Functional complexity of the axonal growth cone: a proteomic analysis." PLoS One **7**(2): e31858.

[20] Tojima, T., J. H. Hines, et al. "Second messengers and membrane trafficking direct and organize growth cone steering." Nat Rev Neurosci **12**(4): 191-203.

[21] Webber, C. A., J. C. Hocking, et al. (2002). "Metalloproteases and guidance of retinal axons in the developing visual system." J Neurosci **22**(18): 8091-8100.

[22] Tharmalingam, S., A. M. Daulat, et al. "Calcium-sensing receptor modulates cell adhesion and migration via integrins." J Biol Chem **286**(47): 40922-40933.

[23] Vernadakis, A. (1988). "Neuron-glia interrelations." Int Rev Neurobiol **30**: 149-224.

[24] Jessen, K. R. (2004). "Glial cells." Int J Biochem Cell Biol **36**(10): 1861-1867.

[25] Nieuwenhuys, R. (1994). "Comparative neuroanatomy: place, principles, practice and programme." Eur J Morphol **32**(2-4): 142-155.

[26] Toyoshima, Y., S. Sekiguchi, et al. "Differentiation of neural cells in the fetal cerebral cortex of cynomolgus monkeys (Macaca fascicularis)." Comp Med **62**(1): 53-60.

[27] Vogiatzis, I., Z. Louvaris, et al. "Frontal cerebral cortex blood flow, oxygen delivery and oxygenation during normoxic and hypoxic exercise in athletes." J Physiol **589**(Pt 16): 4027-4039.

[28] Yeo, B. T., F. M. Krienen, et al. "The organization of the human cerebral cortex estimated by intrinsic functional connectivity." J Neurophysiol **106**(3): 1125-1165.

[29] Yeterian, E. H., D. N. Pandya, et al. "The cortical connectivity of the prefrontal cortex in the monkey brain." Cortex **48**(1): 58-81.

[30] Barbas, H. and D. N. Pandya (1989). "Architecture and intrinsic connections of the prefrontal cortex in the rhesus monkey." J Comp Neurol **286**(3): 353-375.

[31] Toh, M. Y., R. B. Falk, et al. (1996). "Interactive brain atlas with the Visible Human Project data: development methods and techniques." Radiographics **16**(5): 1201-1206.

[32] Jones, E. G. and T. P. Powell (1970). "An anatomical study of converging sensory

pathways within the cerebral cortex of the monkey." Brain **93**(4): 793-820.

[33] Petrides, M. and D. N. Pandya (2007). "Efferent association pathways from the rostral prefrontal cortex in the macaque monkey." J Neurosci **27**(43): 11573-11586.

[34] Petrides, M. and D. N. Pandya (2006). "Efferent association pathways originating in the caudal prefrontal cortex in the macaque monkey." J Comp Neurol **498**(2): 227-251.

[35] Barbas, H. (1993). "Organization of cortical afferent input to orbitofrontal areas in the rhesus monkey." Neuroscience **56**(4): 841-864.

[36] Budd, J. M. and Z. F. Kisvarday "Communication and wiring in the cortical connectome." Front Neuroanat **6**: 42.

[37] Bertram, J. S. (2000). "The molecular biology of cancer." Mol Aspects Med **21**(6): 167-223.

[38] Meng, X., J. Zhong, et al. "A new hypothesis for the cancer mechanism." Cancer Metastasis Rev **31**(1-2): 247-268.

[39] Marie, S. K. and S. M. Shinjo "Metabolism and brain cancer." Clinics (Sao Paulo) **66 Suppl 1**: 33-43.

[40] Wang, D., C. Qiu, et al. "Human microRNA oncogenes and tumor suppressors show significantly different biological patterns: from functions to targets." PLoS One **5**(9).

[41] Kanu, O. O., B. Hughes, et al. (2009). "Glioblastoma Multiforme Oncogenomics and Signaling Pathways." Clin Med Oncol **3**: 39-52.

[42] Moller, H. G., A. P. Rasmussen, et al. "A systematic review of microRNA in glioblastoma multiforme: micro-modulators in the mesenchymal mode of migration and invasion." Mol Neurobiol **47**(1): 131-144.

[43] Ohgaki, H. and P. Kleihues (2007). "Genetic pathways to primary and secondary glioblastoma." Am J Pathol **170**(5): 1445-1453.

[44] Ohgaki, H., P. Dessen, et al. (2004). "Genetic pathways to glioblastoma: a population-based study." Cancer Res **64**(19): 6892-6899.

[45] Ohgaki, H. and P. Kleihues (2005). "Population-based studies on incidence, survival rates, and genetic alterations in astrocytic and oligodendroglial gliomas." J Neuropathol Exp Neurol **64**(6): 479-489.

[46] Furnari, F. B., T. Fenton, et al. (2007). "Malignant astrocytic glioma: genetics, biology, and paths to treatment." Genes Dev **21**(21): 2683-2710.

[47] Zhong, J., A. Paul, et al. "Mesenchymal migration as a therapeutic target in glioblastoma." J Oncol **2010**: 430142.

[48] Frisk, T., S. Rydholm, et al. (2007). "A microfluidic device for parallel 3-D cell cultures

in asymmetric environments." Electrophoresis **28**(24): 4705-4712.

[49] Chung, S., R. Sudo, et al. "Microfluidic platforms for studies of angiogenesis, cell migration, and cell-cell interactions. Sixth International Bio-Fluid Mechanics Symposium and Workshop March 28-30, 2008 Pasadena, California." Ann Biomed Eng **38**(3): 1164-1177.

[50] Knoll, B., C. Weinl, et al. (2007). "Stripe assay to examine axonal guidance and cell migration." Nat Protoc **2**(5): 1216-1224.

[51] Chen, Z. L., V. Haegeli, et al. (2009). "Cortical deficiency of laminin gamma1 impairs the AKT/GSK-3beta signaling pathway and leads to defects in neurite outgrowth and neuronal migration." Dev Biol **327**(1): 158-168.

[52] Kiryushko, D., V. Berezin, et al. (2004). "Regulators of neurite outgrowth: role of cell adhesion molecules." Ann N Y Acad Sci **1014**: 140-154.

[53] Timpl, R. (1996). "Macromolecular organization of basement membranes." Curr Opin Cell Biol **8**(5): 618-624.

[54] Grimpe, B., S. Dong, et al. (2002). "The critical role of basement membrane-independent laminin gamma 1 chain during axon regeneration in the CNS." J Neurosci **22**(8): 3144-3160.

[55] Yin, Y., Y. Kikkawa, et al. (2003). "Expression of laminin chains by central neurons: analysis with gene and protein trapping techniques." Genesis **36**(2): 114-127.

[56] Gomez, T. M. and P. C. Letourneau (1994). "Filopodia initiate choices made by sensory neuron growth cones at laminin/fibronectin borders in vitro." J Neurosci **14**(10): 5959-5972.

[57] Yamaguchi, Y. (2000). "Lecticans: organizers of the brain extracellular matrix." Cell Mol Life Sci **57**(2): 276-289.

[58] Siebert, J. R. and D. J. Osterhout "The inhibitory effects of chondroitin sulfate proteoglycans on oligodendrocytes." J Neurochem **119**(1): 176-188.

[59] Gomez, T. M. and P. C. Letourneau (1994). "Filopodia initiate choices made by sensory neuron growth cones at laminin/fibronectin borders in vitro." J Neurosci **14**(10): 5959-5972.

[60] Chen, Z. L., V. Haegeli, et al. (2009). "Cortical deficiency of laminin gamma1 impairs the AKT/GSK-3beta signaling pathway and leads to defects in neurite outgrowth and neuronal migration." Dev Biol **327**(1): 158-168.

[61] Demuth, T. and M. E. Berens (2004). "Molecular mechanisms of glioma cell migration and invasion." J Neurooncol **70**(2): 217-228.

[62] Martin, S., H. Janouskova, et al. "Integrins and p53 pathways in glioblastoma resistance to temozolomide." Front Oncol **2**: 157.

[63] Wick, W., M. Weller, et al. "Pathway inhibition: emerging molecular targets for treating glioblastoma." Neuro Oncol **13**(6): 566-579.

[64] Gritsenko, P. G., O. Ilina, et al. "Interstitial guidance of cancer invasion." J Pathol **226**(2): 185-199.

[65] Saito, T., S. M. Albelda, et al. (1994). "Identification of integrin receptors on cultured human bone cells." J Orthop Res **12**(3): 384-394.

[66] Yoshizumi, M., J. Abe, et al. (2003). "Stress and vascular responses: atheroprotective effect of laminar fluid shear stress in endothelial cells: possible role of mitogen-activated protein kinases." J Pharmacol Sci 91(3): 172-176.

Biographical Information

Neil Hall was born in Arlington, Texas on June 13th, 1990. He spent the first five years of his life living in Arlington, but moved to Taiwan from age five to age eight for his father's work. At age eight he moved to Allen, Texas where he completed primary school. He then moved to Arlington, Texas and began attending the University of Texas at Arlington where he pursued the 5-year fast-track biomedical engineering B.S./M.S. degree plan. Throughout his time at UT Arlington, he stayed very active on campus, serving as president of three different organizations on campus, and held various jobs including UTA recruitment telecounselor, UTA engineering summer camp lead project mentor, and Emergency Room Medical Scribe. He joined Dr. Young-tae Kim's laboratory in March 2009 as a sophomore in college. After graduating in May of 2013 with his Bachelor's Degree and Master's Degree, he plans on working in the biomedical engineering industry for several years before returning to school to pursue the degrees of M.D. and Ph.D. and work in the field of neuroscience and oncology research.